Journal of Fluorine Chemistry 132 (2011) 216–221

Contents lists available at ScienceDirect

Journal of Fluorine Chemistry

journal homepage: www.elsevier.com/locate/fluor

Direct dynamics studies for the reactions of CF_3CHFCF_3 and $CF_3CF_2CHF_2$ with H atoms

Li Wang, Yuan Zhao, Jinglai Zhang *

Institute of Environmental and Analytical Sciences, College of Chemistry and Chemical Engineering, Henan University, Kaifeng, Henan 475004, PR China

ARTICLE INFO

Article history:
Received 16 November 2010
Received in revised form 12 January 2011
Accepted 20 January 2011
Available online 1 February 2011

Keywords:
CF_3CHFCF_3
$CF_3CF_2CHF_2$
Direct dynamics method
Rate constants

ABSTRACT

The rate constants of the hydrogen abstraction reactions of CF_3CHFCF_3 + H (R1) and $CF_3CF_2CHF_2$ + H (R2) have been calculated by means of the dual-level direct dynamics method. Optimized geometries and frequencies of stationary points and extra points along the minimum-energy path (MEP) are obtained at the MPW1K/6-311+G(d,p) level, and the classical energetic information is further corrected with the interpolated single-point energy (ISPE) approach by the G3(MP2) level of theory. Using the canonical variational transition state theory (CVT) with small-curvature tunneling corrections (SCT), the rate constants are evaluated over a wide temperature range of 200–2000 K. The calculated CVT/SCT rate constants are in good agreement with available experimental values. It is found that the variational effect is very small and almost negligible over the whole temperature region. However, the small-curvature tunneling correction plays an important role in the lower temperature range. Furthermore, the heats of formation of species $CF_3CF_2CHF_2$ (SC_1 or SC_2) and $CF_3CF_2CF_2$ are studied using isodesmic reactions to further elucidate the thermodynamic properties.

1. Introduction

Recognition of the adverse impact of chlorofluorocarbons (CFCs) on stratospheric ozone has prompted an international effort to replace CFCs with environmental friendly alternatives [1,2]. Hydrofluorocarbons (HFCs) were proposed as one of the important candidates to replace CFCs used in refrigeration, air conditioning, foam blowing, and cleaning applications [3,4] over past ten years. They contain neither chlorine atom nor bromine atom and thus, their ozone depletion potentials are virtually zero, though they may contribute to the greenhouse effect because they contain numerous C–F bonds. As the HFCs molecules include at least one C–H bond, they are therefore susceptible to attack by atmospheric constituents. The construction of the reaction mechanism and kinetic data for HFCs is needed not only to estimate their atmospheric lifetimes but also to find their importance in other application [5,6]. In this work, we focus on theoretical investigation on the mechanisms and kinetics of reactions CF_3CHFCF_3 (HFC-227ea) and its isomer $CF_3CF_2CHF_2$ (HFC-227ca) with hydrogen atom. Both HFC-227ea and HFC-227ca have been used as the replacement refrigerant for CFC-114 (CF_2ClCF_2Cl) in centrifugal chillers. Moreover, CF_3CHFCF_3 (HFC-227ea) are considered as a Halon replacement in firefighting applications [7–9]. Owing to their importance, some experimental and theoretical studies [10,11] have been performed on the reactions CF_3CHFCF_3 with OH radical and oxygen atom. On the contrary, limited experimental data is available for the reactions CF_3CHFCF_3 (HFC-227ea) and $CF_3CF_2CHF_2$ (HFC-227ca) with H atom. Yamamoto et al. [12] measured the rate constants for the reactions $CF_3CHFCF_3 + H \rightarrow CF_3CFCF_3 + H_2$ (R1) and $CF_3CF_2CHF_2 + H \rightarrow CF_3CF_2CF_2 + H_2$ (R2) in a temperature range from 1000 to 1180 K by a shock tube technique coupled with atomic resonance absorption spectroscopy (ARAS) and obtained the corresponding rate-temperature expressions (in $cm^3\ mol^{-1}\ s^{-1}$) of $k_1 = 10^{-9.15\pm0.66} \exp[-(63 \pm 14)\ kJ\ mol^{-1}/RT]$ and $k_2 = 10^{-9.44\pm0.32} \exp\ [-(57 \pm 7)\ kJ\ mol^{-1}/RT]$. To evaluate the validity of the experimental results, Yamamoto et al. [12] also calculated the rate coefficients k_1 by using the conventional transition state theory (TST) including the tunneling effect based on the Wigner expression. The TST fitted activation energy (9.8 kcal mol^{-1}) produced great deviation with the experimental value (15.1 ± 3.3 kcal mol^{-1}) from the Arrhenius expression, suggesting that the conventional TST and/or the quantum mechanical tunneling correction based on the Wigner expression used in Ref. [12] to calculate the rate coefficient are very likely inadequate. In addition, the reaction enthalpy and barrier height of R1 were calculated by Lee et al. [13] using *ab initio*, DFT, and IMOMO theory. However, they did not calculate the rate constants of R1. To the best of our knowledge, little theoretical study was performed for reaction R2 except that the barrier heights of (R2a)

* Corresponding author. Tel.: +86 378 3881589.
E-mail address: zhangjinglai@henu.edu.cn (J. Zhang).

0022-1139/$ – see front matter © 2011 Elsevier B.V. All rights reserved.
doi:10.1016/j.jfluchem.2011.01.009

and (R2b) were obtained at the G2(MP2) level [12]. Thus, a detailed theoretical investigation to get more accurate rate constants over a wide temperature range is very desirable.

The molecule CF_3CHFCF_3 has only one stable conformer with C_s symmetry. As to the reactant $CF_3CF_2CHF_2$, it has two stable conformers, SC_1 and SC_2 with C_1 and C_s symmetry, respectively. Based on calculations, SC_1 is stabler than SC_2 by only 0.13 kcal mol^{-1} at the G3(MP2)//MPW1K level. So these two conformers have similar stability and will both contribute to the overall rate constants. The hydrogen-abstraction channels are defined as follows:

$$CF_3CF_2CHF_2(SC_1) + H \rightarrow CF_3CF_2CF_2(C_1) + H_2 \quad (R2a)$$

$$CF_3CF_2CHF_2(SC_2) + H \rightarrow CF_3CF_2CF_2(C_s) + H_2 \quad (R2b)$$

In this paper, we employ dual-level (X//Y) [14,15] direct dynamics method proposed by Truhlar and co-workers [16–18] to investigate the kinetic nature of reactions R1 and R2. The potential energy surface (PES) information is directly obtained by density function theory (DFT) and the rate constants are evaluated by using the variational transition-state theory (VTST) [19–21]. A comparison between theoretical and experimental values is discussed.

In addition, it is well known that the knowledge of the standard enthalpies of formation of the species is important in determining the thermodynamic properties, as well as the kinetics of atmospheric process. However, the thermodynamic data of $CF_3CF_2CHF_2$ (SC_1 and SC_2) and $CF_3CF_2CF_2$ have been little studied experimentally. In the present study, the enthalpies of formation of two species are estimated via two sets of isodesmic reactions.

2. Calculation methods

The equilibrium geometries of all the stationary points (reactants, transition states, and products) involved in the title reactions are optimized by the modified Perdew–Wang 1-parameter model for kinetics (MPW1K) [22] with 6-311+G(d,p) basis set (MPW1K/6-311+G(d,p)). The harmonic vibrational frequencies are calculated to characterize the nature of each critical point at the same level. In order to obtain more reliable reaction enthalpies and barrier heights, higher-level single-point energy calculations for the stationary points are carried out at the G3(MP2) [23] level using the MPW1K-optimized geometries. The minimum energy path (MEP) is calculated by intrinsic reaction coordinate theory (IRC) at the MPW1K/6-311+G(d,p) level to confirm that the transition states really connect with minima along the reaction path. The first and second energy derivatives along the MEP are obtained to calculate the curvature of the reaction path and the generalized vibrational frequencies along the reaction path. The dual-level potential profile along the reaction path is further refined with the interpolated single-point energies (ISPE) method [24], in which a few extra single-point calculations are needed to correct the lower-level reaction path. All the electronic structure calculations are performed by the Gaussian 09 program package [25].

To estimate the enthalpies of formation (ΔH^0_{f298}) of the species $CF_3CF_2CHF_2$ (SC_1 and SC_2) and $CF_3CF_2CF_2$, the following isodesmic reactions are employed.

For $CF_3CF_2CHF_2$ (SC_1 or SC_2)

$$CF_3CF_2CHF_2(SC_1 \text{or} SC_2) + CH_4 \rightarrow CF_3CF_2CH_3 + CH_2F_2 \quad (R3)$$

$$CF_3CF_2CHF_2(SC_1 \text{or} SC_2) + C_2H_6 \rightarrow CF_3CF_2CH_3 + CH_3CHF_2 \quad (R4)$$

For $CF_3CF_2CF_2$

$$CF_3CF_2CF_2 + CH_4 \rightarrow CF_3CF_2CH_3 + CHF_2 \quad (R5)$$

$$CF_3CF_2CF_2 + C_2H_6 \rightarrow CF_3CF_2CH_3 + CH_3CF_2 \quad (R6)$$

By means of the POLYRATE 9.7 program [26], the rate constants are calculated by using the variational transition-state theory (VTST) [19–21] proposed by Truhlar and co-workers. The specific level of VTST we used is canonical variational transition-state theory (CVT) [27–29] with the small-curvature tunneling (SCT) [30,31] method. The generalized normal-mode analysis is carried out in curvilinear coordinates [32,33] so as to lower unphysical imaginary values over a wide range of the reaction coordinate which are obtained with rectilinear coordinates. The curvature components are calculated by using a quadratic fit to obtain the derivative of the gradient with respect to the reaction coordinate.

3. Results and discussion

3.1. Stationary points

The geometric parameters of all the stationary points (reactants, products, and transition states) optimized at the MPW1K/6-311+G(d,p) level are shown in Fig. 1 along with available experimental [34] value. As can be seen from Fig. 1, the calculated bond length of H_2 is the same with the corresponding experimental value. In transition states TS1, TS2a, and TS2b, the breaking C–H bonds are stretched by 24.8%, 25.7%, and 24.8% compared to the C–H equilibrium bond length in isolated CF_3CHFCF_3, $CF_3CF_2CHF_2$ (SC_1), and $CF_3CF_2CHF_2$ (SC_2), respectively. All the forming H–H bonds in three transition states are elongated by 23.0% with respect to the H–H equilibrium bond length in isolated H_2. The elongation of the forming bond (H–H) is almost equal to that of the breaking bond (C–H), indicating that all these H-abstraction reactions proceed via near "symmetrical" barriers.

The harmonic vibrational frequencies are calculated to characterize the nature of each critical point and to make zero-point energy (ZPE) correction. The number of imaginary frequencies (0 or 1) indicates whether a minimum or a transition state has been located. Table 1 lists the harmonic vibrational frequencies of the reactants, products, and transition states calculated at the MPW1K/6-311+G(d,p) level, scaled by a factor of 0.962, along with the experimental value of H_2 [35]. Our calculated frequency of H_2 is in reasonable accord with the experimental value with the deviation of 1.8%. The reactants and products have all real frequencies, while the transition states are confirmed to have only one imaginary frequency. The imaginary frequencies are 1446*i*, 1453*i*, and 1456*i* for TS1, TS2a, and TS2b, respectively. The large value of the imaginary frequency will narrow the width of the potential barrier, and as a result, an important tunneling effect might be found.

Due to lack of the experimental heats of formation of species $CF_3CF_2CHF_2$ (SC_1 or SC_2) and $CF_3CF_2CF_2$, it is difficult to compare calculated reaction enthalpy of R2 with the experimental result. In the present study, their ΔH^0_{f298} values are estimated by two sets of isodesmic reactions (R3)–(R6). The reaction enthalpies of (R3)–(R6) are firstly calculated and then these theoretical results are combined with the known standard enthalpies of formation [36,37] (CH_4, −17.88 kcal mol^{-1}; C_2H_6, −20.0 kcal mol^{-1}; CH_2F_2, −108.2 kcal mol^{-1}; CH_3CHF_2, −120 ± 1 kcal mol^{-1}; $CF_3CF_2CH_3$, −265.79 kcal mol^{-1}; CHF_2, −58 ± 2 kcal mol^{-1}; CH_3CF_2, −71 ± 2 kcal mol^{-1}) to estimate the heats of formation of target species at 298 K. The calculated ΔH^0_{f298} values are tabulated in Table 2. It can be found that the calculated results based on two sets of isodesmic reactions show good consistency. Note that the error limits are calculated by adding the maximum uncertainties of ΔH^0_{f298} values of the reference compounds taken from the literature. The enthalpies of formation are −351.39 ± 1, −351.25 ± 1, and −300.11 ± 2 kcal mol^{-1} for $CF_3CF_2CHF_2$ (SC_1), $CF_3CF_2CHF_2$ (SC_2), and $CF_3CF_2CF_2$, respectively.

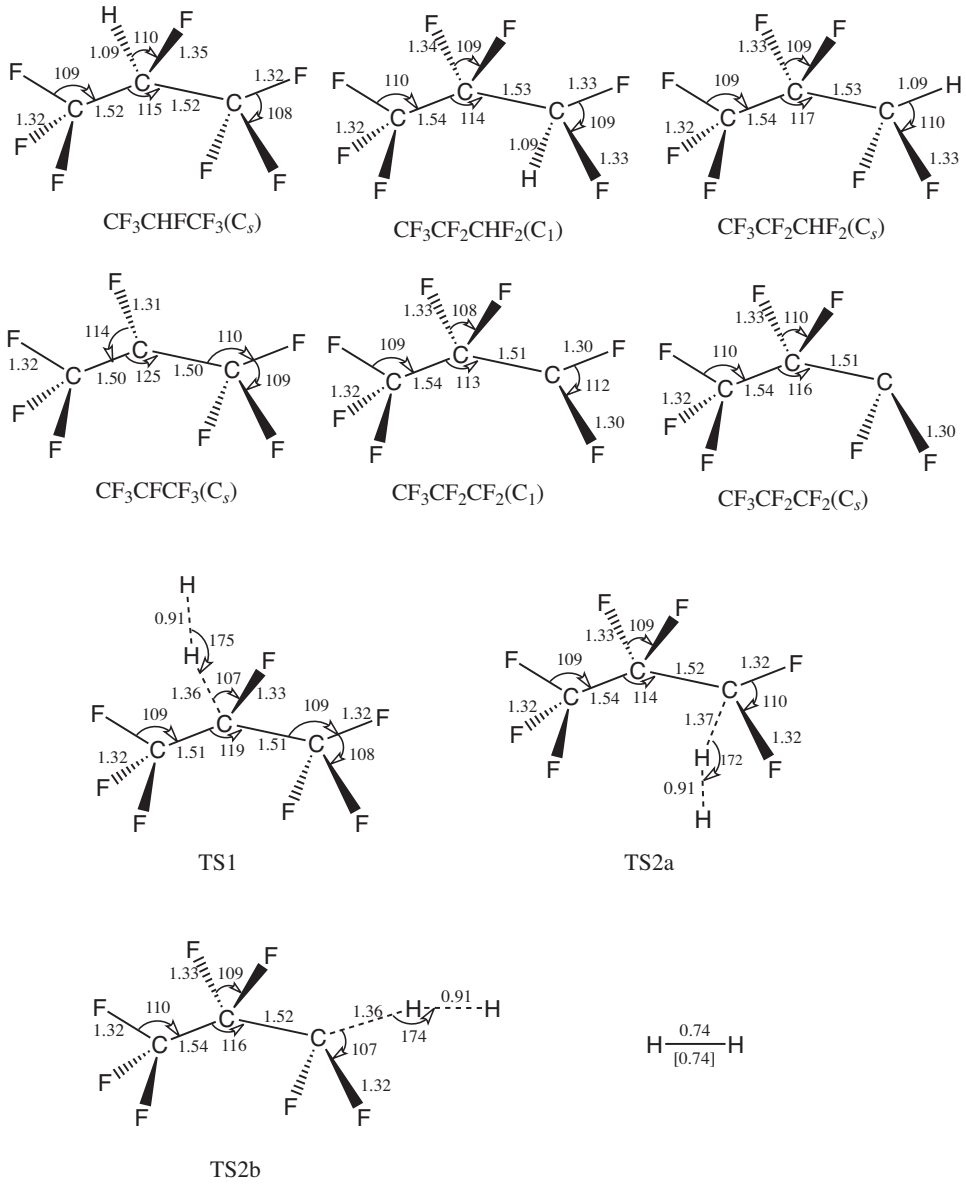

Fig. 1. Optimized geometries of reactants, products, and transition states at the MPW1K/6-311+G(d,p) level. The value in the square bracket is the experimental value [34]. Bond lengths are in angstroms and angles are in degrees.

Table 1
Calculated and experimental frequencies (in cm^{-1}) of the reactants, products, and saddle points at the MPW1K/6-311+G(d,p) level. The computed frequencies are scaled by a factor of 0.962.

	MPW1K/6-311+G(d,p)	Expt.
H_2	4322	4401[a]
CF_3CHFCF_3	3062, 1410, 1391, 1322, 1291, 1261, 1237, 1205, 1157, 1140, 918, 865, 746, 690, 607, 552, 536, 518, 454, 342, 320, 289, 237, 214, 146, 83, 19	
$CF_3CF_2CHF_2$ (SC_1)	3078, 1419, 1389, 1358, 1288, 1261, 1242, 1201, 1163, 1156, 1043, 837, 748, 645, 594, 577, 527, 451, 386, 347, 317, 269, 238, 213, 144, 75, 42	
$CF_3CF_2CHF_2$ (SC_2)	3062, 1443, 1364, 1354, 1264, 1257, 1227, 1214, 1169, 1157, 1113, 785, 708, 614, 604, 564, 523, 502, 371, 367, 334, 276, 217, 205, 146, 88, 23	
CF_3CFCF_3	1430, 1375, 1277, 1227, 1223, 1179, 1165, 997, 783, 707, 668, 615, 552, 539, 500, 458, 346, 318, 294, 248, 166, 135, 49, 15	
$CF_3CF_2CF_2$ (C_1)	1392, 1374, 1319, 1256, 1249, 1206, 1138, 1025, 793, 736, 635, 612, 573, 534, 456, 382, 348, 322, 264, 219, 207, 139, 68, 34	
$CF_3CF_2CF_2$ (C_S)	1396, 1336, 1321, 1252, 1250, 1226, 1171, 1027, 776, 680, 642, 605, 548, 517, 505, 372, 367, 340, 273, 220, 198, 133, 77, 33	
TS1	1446*i*, 1630, 1359, 1356, 1267, 1244, 1220, 1204, 1194, 1127, 1109, 950, 801, 720, 702, 613, 558, 538, 514, 458, 345, 321, 309, 285, 271, 238, 200, 142, 76, 30	
TS2a	1453*i*, 1670, 1375, 1346, 1286, 1253, 1234, 1211, 1174, 1138, 1116, 1027, 789, 731, 643, 607, 577, 532, 451, 389, 347, 321, 297, 278, 261, 225, 209, 142, 72, 38	
TS2b	1456*i*, 1634, 1361, 1342, 1285, 1248, 1244, 1223, 1169, 1144, 1141, 1044, 776, 689, 633, 604, 557, 524, 505, 373, 371, 338, 283, 280, 255, 219, 202, 138, 81, 26	

[a] From Ref. [35].

Table 2
Calculated enthalpies of formation at 298 K (in kcal mol^{-1}).

	G3(MP2)//MPW1K/6-311+G(d,p)	Average value and deviation
$CF_3CF_2CHF_2$ (SC_1) + CH_4	−351.85	−351.39 ± 1.0
$CF_3CF_2CHF_2$ (SC_1) + C_2H_6	−350.94 ± 1.0	
$CF_3CF_2CHF_2$ (SC_2) + CH_4	−351.71	−351.25 ± 1.0
$CF_3CF_2CHF_2$ (SC_2) + C_2H_6	−350.80 ± 1.0	
$CF_3CF_2CF_2$ + CH_4	−300.12 ± 2.0	−300.11 ± 4.0
$CF_3CF_2CF_2$ + C_2H_6	−300.09 ± 2.0	

The reaction enthalpies (ΔH^0_{298}) and barrier heights (ΔE (0 K)) calculated at the MPW1K/6-311+G(d,p) and G3(MP2)//MPW1K/6-311+G(d,p) levels are displayed in Table 3. The calculated reaction enthalpy of R1 (−1.5 kcal mol^{-1}) is considerably lower than the experimental value (−5.93 kcal mol^{-1}) derived from the experimental standard heats of formation (CF_3CHFCF_3, −365.55 kcal mol^{-1}; CF_3CFCF_3, −319.38 kcal mol^{-1}; H, 52.1 kcal mol^{-1}) [36,38]. However, our calculated result agrees well with the *ab initio* benchmark value (−0.7 ± 0.7 kcal mol^{-1}) [13] reported by Lee et al. recently. They also calculated the barrier height using several DFT and *ab initio* methods and obtained the benchmark value 13.3 ± 0.5 kcal mol^{-1} [13], which agree well with the barrier height (11.78 kcal mol^{-1}) calculated at the G3(MP2)//MPW1K/6-311+G(d,p) level. Moreover, it can be found in Table 3 that the barrier heights indicate good agreement with the G2(MP2) values for all three reaction channels. Because of the good agreement between our results and the values obtained by other theoretical methods for both reaction enthalpy (ΔH^0_{298}) and barrier height (ΔE (0 K)), it can be inferred that the potential energy profiles refined at the G3(MP2)//MPW1K/6-311+G(d,p) level are reliable.

The minimum energy path for each reaction is calculated by the intrinsic reaction coordinate (IRC) theory at the MPW1K/6-311+G(d,p) level, and the kinetic calculations of the title reactions are carried out with the VTST-ISPE method at the G3(MP2)//MPW1K level. The classical potential energy ($V_{MEP}(s)$), the ground-state vibrational adiabatic potential energy $V^G_a(s)$, and the zero-point energy (ZPE) curves of reaction as functions of the intrinsic reaction coordinate (s) for R1 are plotted in Fig. 2, where the ground-state vibrationally adiabatic potential curve is defined as $V^G_a(s) = V_{MEP}(s) + ZPE(s)$. The maximum positions of $V^G_a(s)$ and $V_{MEP}(s)$ curves are the same, which implies that the variational effect will be small or almost negligible. The small variational effect on the rate constant will be confirmed in the following section. However, the variational effect becomes important for reaction channels (R2a) and (R2b).

3.2. Kinetics calculations

Since the rate constants estimated by the conventional TST with the tunneling effect based on the Wigner expression in Ref. [12] are inadequate, VTST calculation are required. In this paper, dual-level (X//Y) direct dynamics calculations are carried out for the title reactions using the variational transition-state theory with the interpolated single-point energies (VTST-ISPE) approach. The PES information for each reaction obtained at the G3(MP2)//MPW1K/6-311+G(d,p) level is put into POLYRATE 9.7 program to calculate the VTST rate constants over a temperature range from 200 to 2000 K. The forward rate constants for the title hydrogen abstraction reactions are calculated by conventional transition state theory (TST), canonical variational transition state theory (CVT), and CVT with a small-curvature tunneling correction (CVT/SCT).

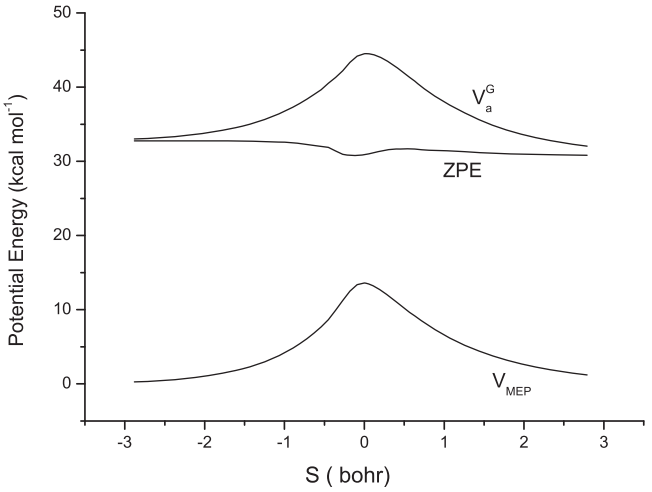

Fig. 2. Classical potential energy curve (V_{MEP}), ground-state vibrationally adiabatic energy curve (V^G_a), and zero-point-energy curve ZPE as functions of s bohr at the G3(MP2)//MPW1K/6-311+G(d,p) level for the reaction $CF_3CHFCF_3 + H \rightarrow CF_3CFCF_3 + H_2$ (R1).

The TST, CVT, and CVT/SCT rate constants of R1 as well as the corresponding experimental values [12] are presented in Fig. 3. As can be seen from Fig. 3, the rate constants of TST and CVT are nearly the same over the whole calculated temperature region, which means that the variational effect on the rate constants is very small or almost negligible. The ratios of $k_{CVT/SCT}/k_{CVT}$ are 2733, 31, 1.5, and 1.05 at 200 K, 300 K, 800 K, and 2000 K, respectively, indicating that small-curvature tunneling (SCT) correction should be taken into account especially in the lower temperatures. It is consistent with the result that the imaginary vibrational frequency of TS1 is large. Similar behavior can be drawn from other two reaction channels. The agreement of the calculated CVT/SCT rate constants and experimental data is reasonably good, where the root mean squared error is 1.84 in the temperature range of 1000–1180 K. The calculated activation energy of 13.74 kcal mol^{-1} is in reasonable agreement with the corresponding experimental value of 15.1 ± 3.3 kcal mol^{-1} in the temperature range 1000–1180 K [12], respectively. Furthermore, the present results calculated by dual-level direct dynamics method match better with the experimental ones than

Table 3
Enthalpies (in kcal mol^{-1}) and barrier heights (in kcal mol^{-1}) at the MPW1K/6-311+G(d,p), G3(MP2)//MPW1K/6-311+G(d,p), available experimental values, and theoretical data.

	CF_3CHFCF_3 + H		$CF_3CF_2CHF_2$ (SC_1) + H		$CF_3CF_2CHF_2$ (SC_2) + H	
	ΔH^0_{298}	ΔE (0 K)	ΔH^0_{298}	ΔE (0 K)	ΔH^0_{298}	ΔE (0 K)
MPW1K/6-311+G(d,p)	−1.21	10.81	−0.67	11.12	−1.15	10.34
G3(MP2)//MPW1K/6-311+G(d,p)	−1.5	11.78	−1.83	12.09	−2.47	11.43
Expt.	−5.93[a]	12.6 ± 3.1[a]		12.85[a]		12.13[a]
	−0.7 ± 0.7[b]	13.3 ± 0.5[b]				

[a] From Ref. [12].
[b] From Ref. [13].

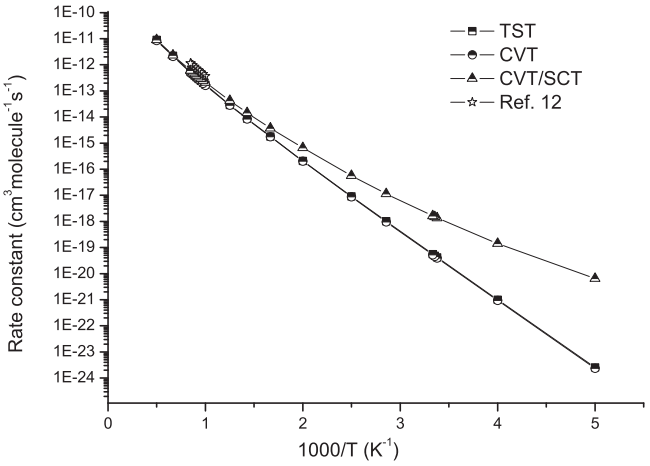

Fig. 3. Plot of the TST, CVT, and CVT/SCT rate constants calculated at the G3(MP2)//MPW1K/6-311+G(d,p) level along with the available experimental values versus 1000/T between 200 and 2000 K for the title reaction $CF_3CHFCF_3 + H \rightarrow CF_3CFCF_3 + H_2$ (R1).

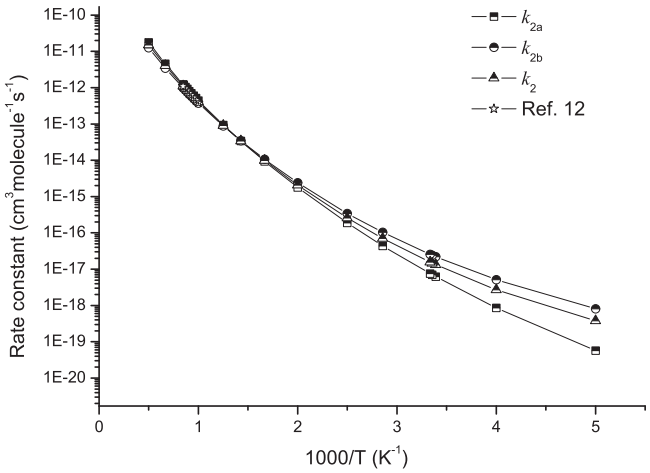

Fig. 4. Plot of the CVT/SCT rate constants calculated at the G3(MP2)//MPW1K/6-311+G(d,p) level along with the available experimental values versus 1000/T between 200 and 2000 K for the title reaction $CF_3CF_2CHF_2 + H \rightarrow CF_3CF_2CF_2 + H_2$ (R2).

the values obtained by the conventional TST including the tunneling effect based on the Wigner expression by Yamamoto et al. [12].

As to the reactant $CF_3CF_2CF_2H$, the energy of SC_1 is much close to that of SC_2, so they will both contribute to the overall rate constants. The total rate constants (k_2) can be obtained from the following expression: $k_2 = \omega_1 k_{2a} + \omega_2 k_{2b}$ where ω_1 and ω_2 are the weight factors of each conformer calculated from the Boltzmann distribution function, and k_{2a} and k_{2b} are the rate constants for the hydrogen abstraction from the SC_1 and SC_2 conformers of $CF_3CF_2CHF_2$. The calculated CVT/SCT rate constants and available experimental date [12] for R2 are drawn in Fig. 4, and the CVT/SCT rate constants of R1, R2, and the corresponding experiment values [12] are tabulated in Table 4. The calculated CVT/SCT rate constants of R2 are in excellent agreement with the corresponding experimental data in the temperature range of 1000–1180 K. Moreover, the Arrhenius expression of $k_2 = 2.87 \times 10^{-10} \exp(-54.5\ \text{kJ mol}^{-1}/RT)\ \text{cm}^3\ \text{mol}^{-1}\ \text{s}^{-1}$ fitted by the CVT/SCT rate constant in a temperature range of 1000–1180 K is in good accord with that reported by Yamamoto et al. [12], $k_2 = 10^{-9.44\pm0.32} \exp[-(57 \pm 7)\ \text{kJ mol}^{-1}/RT]$ (in $\text{cm}^3\ \text{mol}^{-1}\ \text{s}^{-1}$).

Therefore, it is reasonable to believe that the present calculations can provide reliable predictions of the rate constants for the title reactions during a large temperature region, which will be useful for the atmospheric modeling calculations and help to assess their atmospheric lifetimes of HFCs. Thus for the convenience of future experimental measurements, the CVT/SCT rate constants of R1 and R2 are firstly fitted to the popular modified Arrhenius expression, $k = AT^n \exp(-E/RT)$, where A, n, and E are fitting parameters and R is the gas constant. This equation is labeled model 1 in this paper. Model 1 has been usded widely for fitting theoretical rate constants in the literature [39–41]. Recently, Truhlar et al. [42] proposed a new model with one more parameter to give small fitting error and have the correct low-temperature asymptotic behavior for activation energy and rate constant, which

Table 4
The CVT/SCT rate constants (in $\text{cm}^3\ \text{mol}^{-1}\ \text{s}^{-1}$) and experimental values for the reactions R1 and R2 in a temperature range of 200–2000 K.

T (K)	k_1	$k_{expt.}$[a]	k_{2a}	k_{2b}	k_2	$k_{expt.}$[a]
200	6.45×10^{-21}		5.69×10^{-20}	8.14×10^{-19}	3.76×10^{-19}	
250	1.42×10^{-19}		8.61×10^{-19}	5.10×10^{-18}	2.71×10^{-18}	
296	1.36×10^{-18}		6.18×10^{-18}	2.19×10^{-17}	1.32×10^{-17}	
298	1.49×10^{-18}		6.96×10^{-18}	2.40×10^{-17}	1.46×10^{-17}	
300	1.63×10^{-18}		7.52×10^{-18}	2.55×10^{-17}	1.56×10^{-17}	
350	1.15×10^{-17}		4.37×10^{-17}	1.03×10^{-16}	7.07×10^{-17}	
400	5.70×10^{-17}		1.87×10^{-16}	3.42×10^{-16}	2.58×10^{-16}	
500	6.59×10^{-16}		1.78×10^{-15}	2.40×10^{-15}	2.07×10^{-15}	
600	3.74×10^{-15}		9.36×10^{-15}	1.06×10^{-14}	9.95×10^{-15}	
700	1.45×10^{-14}		3.38×10^{-14}	3.43×10^{-14}	3.40×10^{-14}	
800	4.23×10^{-14}		9.40×10^{-14}	8.86×10^{-14}	9.14×10^{-14}	
1000	2.10×10^{-13}	3.63×10^{-13}	4.41×10^{-13}	3.76×10^{-13}	4.10×10^{-13}	3.82×10^{-13}
1025	2.48×10^{-13}	4.36×10^{-13}	5.17×10^{-13}	4.37×10^{-13}	4.78×10^{-13}	4.52×10^{-13}
1050	2.90×10^{-13}	5.20×10^{-13}	6.02×10^{-13}	5.05×10^{-13}	5.55×10^{-13}	5.30×10^{-13}
1075	3.37×10^{-13}	6.15×10^{-13}	6.98×10^{-13}	5.80×10^{-13}	6.41×10^{-13}	6.17×10^{-13}
1100	3.90×10^{-13}	7.22×10^{-13}	8.04×10^{-13}	6.63×10^{-13}	7.36×10^{-13}	7.13×10^{-13}
1125	4.49×10^{-13}	8.41×10^{-13}	9.22×10^{-13}	7.55×10^{-13}	8.41×10^{-13}	8.19×10^{-13}
1150	5.15×10^{-13}	9.74×10^{-13}	1.05×10^{-12}	8.55×10^{-13}	9.55×10^{-13}	9.35×10^{-13}
1175	5.87×10^{-13}	1.12×10^{-12}	1.20×10^{-12}	9.65×10^{-13}	1.09×10^{-12}	1.06×10^{-12}
1180	6.02×10^{-13}	1.15×10^{-12}	1.23×10^{-12}	9.88×10^{-13}	1.11×10^{-12}	1.09×10^{-12}
1500	2.30×10^{-12}		4.57×10^{-12}	3.45×10^{-12}	4.02×10^{-12}	
2000	8.98×10^{-12}		1.76×10^{-11}	1.26×10^{-11}	1.51×10^{-11}	

[a] From Ref. [12].

Table 5
The fitted parameters using two modified Arrhenius equations for reactions R1 and R2 for temperature from 200 K to 2500 K.

Parameters	R1	R2
Mode 1		
$k = AT^n \exp(-E/RT)$		
A (s^{-1})	3.70×10^{-25}	3.40×10^{-28}
n	4.29	5.22
E (kcal mol^{-1})	5.35	2.96
RMSR	0.18	0.24
Mode 2		
$k = AT^n \exp[-E(T+T_0)/R(T^2+T_0^2)]$		
A (s^{-1})	1.02×10^{-19}	3.82×10^{-22}
n	2.63	3.37
E (kcal mol^{-1})	6.28	4.36
T_0 (K)	179.7	191.4
RMSR	0.07	0.10

is called Model 2. The model 2 rate constant expression is $k = AT^n \exp[-E(T+T_0)/R(T^2+T_0^2)]$, where A, n, E, and T_0 are fitting parameters and R is the gas constant. The fitting results are presented in Table 5. It can be found that the model 2 reduces the fitting error compared to model 1 over a wide range of temperature for both reactions.

4. Conclusion

The hydrogen abstraction reactions of CF_3CHFCF_3 + H (R1) and $CF_3CF_3CHF_2$ + H (R2) are studied theoretically by a dual-level direct dynamics method in the present work. The rate constants calculated by the canonical variational transition state theory (CVT) with a small curvature tunneling correction (SCT) are observed to agree well with the available experimental values. The variational effect is very small and almost negligible over the whole temperature region for reaction R1, whereas it becomes important for reaction channels (R2a) and (R2b). The small-curvature tunneling effect plays an important role in the lower temperature range. Two models are used to fit rate constants in a temperature range of 200–2000 K. Furthermore, the heats of formation of species $CF_3CF_2CHF_2$ (SC_1 or SC_2) and $CF_3CF_2CF_2$ are studied using isodesmic reactions at the G3(MP2)//MPW1K/6-311+G(d,p) level.

Acknowledgments

We thank Professor Donald G. Truhlar for providing the POLYRATE 9.7 program. This work was supported by the National Natural Science Foundation of China (21003036), Science Foundation of Henan Province (2008A150005, 2011B150003), Science Foundation of Henan University (2009YBZR013, SBGJ090507), Doctor Foundation of Henan University.

References

[1] A. Talhaoui, F. Louis, P. Devolder, B. Meriaux, J.P. Sawerysyn, M.T. Rayez, J.C. Rayez, J. Phys. Chem. 100 (1996) 13531–13538.
[2] R. Liu, R.E. Huie, M.J. Kurylo, J. Phys. Chem. 94 (1990) 3247–3249.
[3] K. Stemmler, D. Folini, S. Ubl, M.K. Vollmer, S. Reimann, S. O'Doherty, B.R. Greally, P.G. Simmonds, A.J. Manning, Environ. Sci. Technol. 41 (2007) 1145–1151.
[4] M.K. Vollmer, S. Reimann, D. Folini, L.W. Porter, L.P. Steele, Geophys. Res. Lett. 33 (2006) L20806, doi:10.1029/2006GL026763.
[5] J. Pu, D.G. Truhlar, J. Phys. Chem. A 109 (2005) 773–778.
[6] Y. Zhao, B.J. Lynch, D.G. Truhlar, Phys. Chem. Chem. Phys. 7 (2005) 43–52.
[7] D. Jager, M. Manning, L. Kuijpers, et al., IPCC/TEAP Special Report on Safeguarding the Ozone Layer and the Global Climate System: Issues related to Hydrofluorocarbons and Perfluorocarbons, Cambridge University Press, Cambridge, 2005.
[8] J.-Y. Park, J.S. Lim, B.G. Lee, Y.W. Lee, Int. J. Thermophys. 22 (2001) 901–917.
[9] F. Gui, D.D. Buck, R.P. Scaringe, L.R. Grzyll, J.M. Gottschlich, in: Proceedings of the Intersociety Energy Conversion Engineering Conference, vol. 2, IEEE, Piscataway, NJ, (1996), p. 1355.
[10] J.-Y. Liu, Z.-S. Li, Z.-W. Dai, X.-R. Huang, C.-C. Sun, Chem. Phys. Lett. 362 (2002) 39–46.
[11] J.-Y. Liu, Z.-S. Li, Z.-W. Dai, X.-R. Huang, C.-C. Sun, Chem. Phys. 286 (2003) 173–180.
[12] O. Yamamoto, K. Takahashi, T. Inomata, J. Phys. Chem. A 108 (2004) 1417–1424.
[13] E.P.F. Lee, J.M. Dyke, W.K. Chow, F.T. Chau, D.K.W. Mok, J. Comput. Chem. 28 (2007) 1582–1592.
[14] W.-P. Hu, Y.-P. Liu, D.G. Truhlar, J. Chem. Soc. Faraday Trans. 90 (1994) 1715–1725.
[15] J.C. Corchado, E.L. Coitiño, Y.-Y. Chuang, P.L. Fast, D.G. Truhlar, J. Phys. Chem. A 102 (1998) 2424–2438.
[16] D.G. Truhlar, in: D. Heidrich (Ed.), The Reaction Path in Chemistry: Current Approaches and Perspectives, Kluwer, Dordrecht, The Netherlands, 1995, p. 229.
[17] W.P. Hu, D.G. Truhlar, J. Am. Chem. Soc. 118 (1996) 860–869.
[18] D.G. Truhlar, B.C. Garrett, S.J. Klippenstein, J. Phys. Chem. 100 (1996) 12771–12800.
[19] D.G. Truhlar, B.C. Garrett, Acc. Chem. Res. 13 (1980) 440–448.
[20] D.G. Truhlar, A.D. Isaacson, B.C. Garrett, in: M. Baer (Ed.), The Theory of Chemical Reaction Dynamics, CRC Press, Boca Raton, FL, 1985, p. 65.
[21] D.G. Truhlar, B.C. Garrett, Annu. Rev. Phys. Chem. 35 (1984) 159–189.
[22] B.J. Lynch, D.G. Truhlar, J. Phys. Chem. A 105 (2001) 2936–2941.
[23] L.A. Curtiss, P.C. Redfern, K. Raghavachari, V. Rassolov, J.A. Pople, J. Chem. Phys. 110 (1999) 4703–4709.
[24] Y.Y. Chuang, J.C. Corchado, D.G. Truhlar, J. Phys. Chem. 103 (1999) 1140–1149.
[25] M.J. Frisch, G.W. Trucks, H.B. Schlegel, et al., Gaussian 09 Revision A.02, Gaussian, Inc., Wallingford, CT, 2009.
[26] J.C. Corchado, Y.Y. Chuang, P.L. Past, W.P. Hu, Y.P. Liu, G.C. Lynch, K.A. Nguyen, C.F. Jackels, A. Fernandez-Ramos, B.A. Ellingson, B.J. Lynch, J.J. Zheng, V.S. Melissas, J. Villa, I. Rossi, E.L. Coitino, J.Z. Pu, T.V. Albu, R. Steckler, B.C. Garrett, A.D. Isaacson, D.G. Truhlar, POLYRATE, version 9.7, University of Minnesota, Minneapolis, 2007.
[27] B.C. Garrett, D.G. Truhlar, J. Chem. Phys. 70 (1979) 1593–1598.
[28] B.C. Garrett, D.G. Truhlar, J. Am. Chem. Soc. 101 (1979) 4534–4548.
[29] B.C. Garrett, D.G. Truhlar, R.S. Grev, A.W. Magnuson, J. Phys. Chem. 84 (1980) 1730–1748.
[30] D.H. Lu, T.N. Truong, V.S. Melissas, G.C. Lynch, Y.P. Liu, B.C. Garrett, R. Steckler, A.D. Issacson, S.N. Rai, G.C. Hancock, J.G. Lauderdale, T. Joseph, D.G. Truhlar, Comput. Phys. Commun. 71 (1992) 235–262.
[31] Y.-P. Liu, G.C. Lynch, T.N. Truong, D.-H. Lu, D.G. Truhlar, B.C. Garrett, J. Am. Chem. Soc. 115 (1993) 2408–2415.
[32] C.F. Jackels, Z. Gu, D.G. Truhlar, J. Chem. Phys. 102 (1995) 3188–3201.
[33] Y.-Y. Chuang, D.G. Truhlar, J. Phys. Chem. 101 (1997) 3808–3814.
[34] G.W.C. Kaye, T.H. Laby, Tables of Physical and Chemical Constants, Longman Group Limited, 1995.
[35] M.W. Chase Jr., J. Phys. Chem. Ref. Data Monograph 9 (1998) 1–1951 (NIST-JANAF Themochemical Tables, 4th ed.).
[36] W.B. DeMore, S.P. Sander, S.P. Golden, C.J. Howard, D.M. Golden, C.E. Kolb, R.F. Hampson, M.J. Molina, Chemical Kinetics and Photochemical Data for Use in Stratospheric Modeling, JPL Publication 97-4, 1997.
[37] A. Vatani, M. Mehrpooya, F. Gharagheizi, Int. J. Mol. Sci. 8 (2007) 407–432.
[38] R.G. Hynes, J.C. Mackie, A.R. Madri, Combust. Flame 113 (1998) 554–565.
[39] H. Gao, Y. Wang, S.-Q. Wan, J.-Y. Liu, C.-C. Sun, J. Mol. Struct.: THEOCHEM 913 (2009) 107–116.
[40] H.-X. Liu, Y. Wang, L. Yang, J.-Y. Liu, H. Gao, Z.-S. Li, C.-C. Sun, J. Comput. Chem. 30 (2009) 2194–2204.
[41] L. Wang, Y. Zhao, J. Zhang, Y.N. Dai, J.-L. Zhang, Theor. Chem. Acc. 128 (2011) 183–189.
[42] J.-J. Zheng, Donald G. Truhlar, Phys. Chem. Chem. Phys. 12 (2010) 7782–7793.